WCTE 2014 Quebec City Canada August 10-14
World Conference on Timber Engineering

DISTRIBUTION OF CHORD FORCES IN LARGE PANELIZED WOOD ROOF DIAPHRAGMS

Weichiang Pang[1], Chun Ni[2], John Lawson[3], Sami Pant[4]

ABSTRACT: Flexible wood roof diaphragms are very common in the United States, both for residential buildings and large-scale commercial buildings. Due to its simplicity, the traditional diaphragm design method is commonly used in diaphragm design, in particular for the design of diaphragms with relatively small dimensions. The traditional diaphragm design method assumes the axial chord forces developed in framing members under in-plane loading are carried only by the perimeter elements. This method has always been thought to be a conservative design method, especially when applied to large diaphragms. In recent years, the engineering community began to question the applicability of the traditional diaphragm design method. A new design approach known as the collective chord design method was proposed to analyze the chord forces for very large flexible roof diaphragms. This method utilizes strain compatibility of a simple beam to estimate the axial forces in multiple chord members. This paper evaluates the applicability of the traditional and collective chord design methods by modeling the behavior of large panelized roof diaphragms numerically.

KEYWORDS: Flexible Roof Diaphragm, Diaphragm Design, Collective Chord Method, Chord Forces

1 INTRODUCTION

Large flexible roof diaphragms are very common in tilt-up concrete construction for big-box retail stores and warehouses, sometimes exceeding of one million square feet [1]. These large roof diaphragms typically consist of either metal decking or wood structural panels on low-slope open-web steel joists or an all-wood system. Due to the sheer size of these large diaphragms, the design and construction of large flexible diaphragms pose many engineering challenges. One of the faster and more cost-effective ways to build very large roof diaphragms is the panelized roof construction method. A panelized roof system may be made up of an all-wood system or a hybrid system consisting of wood structural panels and open-web steel joists (purlins) and joist-girders. In panelized roof construction, the sheathing panels are first assembled on the ground and the pre-fabricated panelized subassemblies are then lifted into place. Each panelized roof subassembly consists of oriented strand board (OSB) or plywood panels attached to a set of wood subpurlins (stiffeners) which are then attached to a single purlin (see Fig. 1). These pre-framed panelized units are lifted into position on the roof and assembled together by connecting the subpurlins to purlins, purlins to girders, and then finally the panel nailing along three edges of each pre-framed unit is performed. This construction method is not only cost effective and fast; it is also one of the safest construction techniques. Since most of the assembly work is performed on the ground, workers spend a minimal amount of time on the roof; hence minimizing the possibility of serious accident. While large panelized roof systems offer many benefits, the actual behavior of these large diaphragms is not fully understood and may be different from the design assumptions commonly employed by engineers for conventional smaller flexible diaphragms.

[1] Weichiang Pang, Clemson University, Clemson, South Carolina, 29634-0911, USA. Email: wpang@clemson.edu
[2] Chun Ni, FPInnovations, Vancouver, BC, Canada.
[3] John Lawson, California Polytechnic State University, San Luis Obispo, USA.
[4] Pant Sami, Clemson University, Clemson, SC, USA.

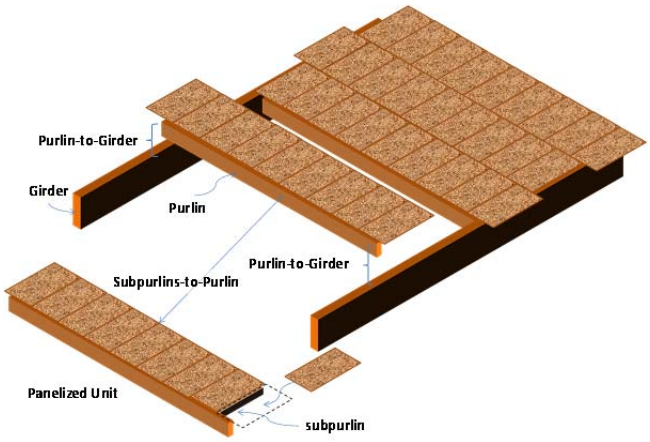

Figure 1: *Panelized roof construction.*

2 DESIGN METHODS

Fig. 2 depicts a roof diaphragm under lateral loads (e.g. earthquake and wind loads). For design purposes, a diaphragm is typically modelled as a simply supported flat "beam".

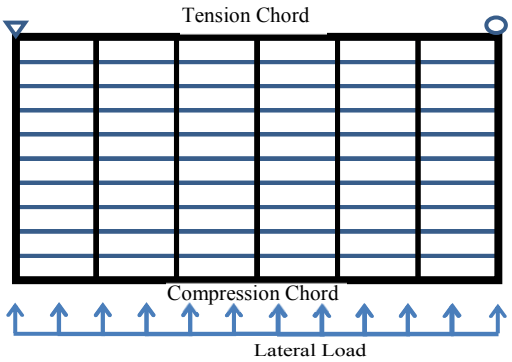

Figure 2: *A roof diaphragm under lateral load, modelled as a simply supported "beam".*

2.1 Traditional Diaphragm Design Method

The traditional diaphragm design method assumes that the axial chord forces developed from flexural behavior due to in-plane lateral loads, such as those due to earthquakes, are carried only by the perimeter elements (Fig. 3). While this approach simplifies the design process, the assumptions used in the traditional approach to analyze the chord forces may not be applicable to very large diaphragms. Starting approximately two decades ago, some in the engineering community began to question the applicability of the traditional chord model for large diaphragms [2][3]. For instance, assuming that the interior continuous elements do not participate as chords may lead to excessively high axial force demands in the perimeter chords, resulting in unrealistically large sizes for framing and connections. As a result, this may lead to an overly conservative and uneconomical design. Thus, for a large roof diaphragm system, a more rigorous analysis of the distribution of forces in the framing members may be warranted.

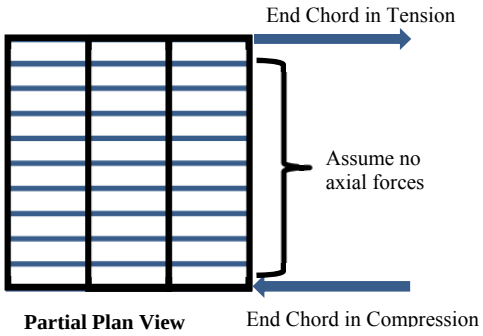

Figure 3: *Chord force distribution based on traditional diaphragm design method.*

2.2 Collective Chord Method

A different design method known as the collective chord design method [3] was proposed for analyzing the chord forces in diaphragms to increase efficiency and potentially accuracy. According to this design method, the continuous framing members within a diaphragm may function as collective chords, which are capable of carrying significant amount of loads. The collective chord method utilizes strain compatibility to estimate the forces in perimeter and intermediate chord members. According to this method, the axial force carried by each continuity chord (or tie) is proportional to its distance from the neutral axis (Fig. 4). Since the interior chords also participate in resisting the diaphragm's flexural behavior, the axial forces in the perimeter chords computed using the collective chord design method could be significantly smaller than that of the traditional design method. While the collective chord design method may yield designs that are more economical than that of the traditional design approach, the collective chord design assumptions have not been rigorously

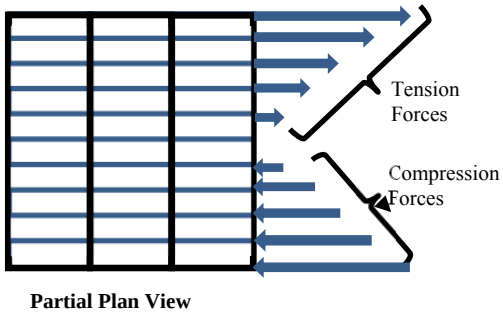

Figure 4: *Chord force distribution based on traditional diaphragm design method.*

evaluated and verified. This paper examines the applicability of the collective chord design method by modeling the behavior of large panelized roof diaphragms numerically.

3 DIAPHRAGM MODEL

The large diaphragm models utilized in this study were created using software called M-CASHEW (Matlab - Cyclic Analysis of SHEar Walls) which was initially developed for modeling light-frame wood shear walls [4]. As part of this study, the M-CASHEW program was modified to include new features for modeling large panelized diaphragms. Fig. 5 outlines the sub-assemblies of a typical large panelized roof diaphragm system. For modeling purposes, the sub-assemblies of a diaphragm were grouped into three main components: framing members, sheathing panels and connectors (i.e. nails and continuity ties). The framing members include the girders, purlins and subpurlins. In this study, the two-node frame (beam) element was used to model the framing members. The sheathing panels were modeled using a specialized membrane element. Two types of zero-length link elements were utilized to model the connectors, namely panel-to-frame (P2F) and frame-to-frame (F2F) elements. The P2F elements were used to model the shear slip behavior of sheathing nails, used to connect the panels to the frames. The F2F elements were used to model (1) the bearing contact between the framing members, (2) the continuity ties (e.g. purlin-to-purlin and girder-to-girder ties), and (3) the connections between subpurlins and purlins. Past studies (e.g. [5]) have shown that the overall behavior of diaphragms and light-frame wood shear walls are mainly governed by the nonlinear shear slip responses of the connectors. Hence, nonlinear link elements were used to model the connectors while the framing members and sheathing panels were modeled using linear elastic elements.

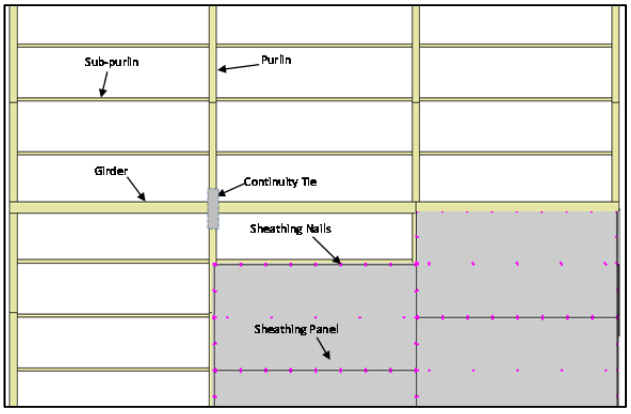

Figure 5. *A section of a panelized roof diaphragm.*

3.1 Frame Element

The girders, purlins and subpurlins were modeled using a two-node frame element with a co-rotational formulation to account for geometric nonlinearity. Each node has three DOFs, two translations and one rotation (Fig. 6). An interpolation matrix with dimensions of 3x6 was used to relate the panel deformations to the deformations of any arbitrary connection points within the frame element [4].

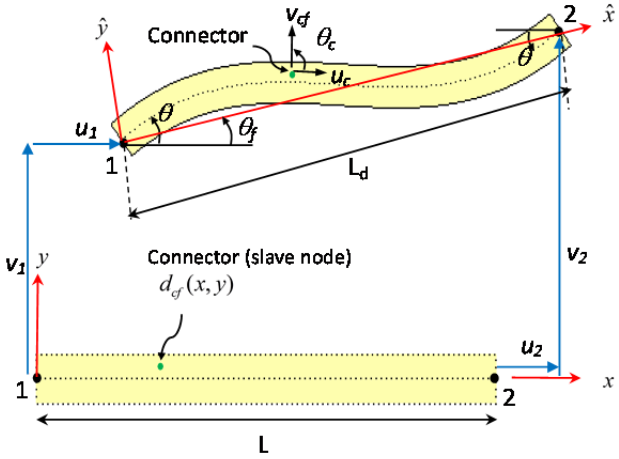

Figure 6. *Kinematics of frame element.*

3.2 Sheathing Element

The sheathing panels in a diaphragm resist mainly the in-plane shear developed due to lateral loading. A specialized shear panel element with five DOFs (Fig. 7), one rigid body rotation, two rigid body translations and two in-plane shear deformations, was formulated and used to model the sheathing [4].

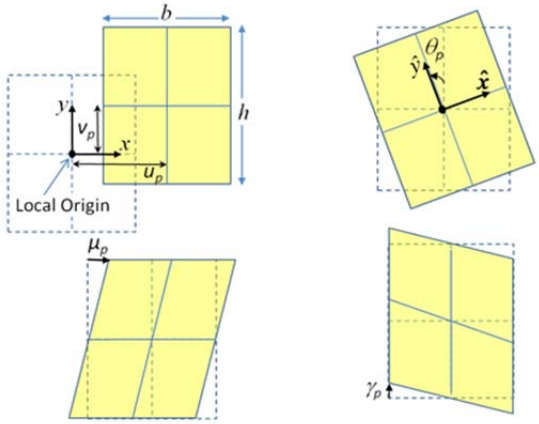

Figure 7. *Kinematics of panel element.*

3.3 Connector Elements

In large diaphragms, the framing system and sheathing panels are assembled together using dowel type

connections (nails, screws and bolts) and metal connectors (i.e. metal splices and continuity ties). Two types of zero-length link elements were formulated to model the connection properties. These two link elements were the frame-to-frame (F2F) and panel-to-frame (P2F) link elements. The general formulations of the F2F and P2F are the same. The link element has two nodes and three DOFs. The three DOFs are characterized by three orthogonal and uncoupled springs, one rotational (k_r) and two translational (k_x and k_y) springs.

3.4 Sheathing Nail

The panel-to-frame (P2F) element was used to model the load-slip response of sheathing nails. The translational DOFs (k_x and k_y) were modeled using the modified Stewart (MSTEW) hysteretic spring, also known as the CUREE hysteretic model [6] (Fig. 8). The MSTEW model consists of ten modeling parameters (K_o, r_1, r_2, r_3, r_4, F_o, F_i, δ_u, α and β). In this study, the sheathing nail parameters used were fitted from the cyclic test data for 10d common nail with 7/16" OSB [7]. Since the moment resistance of

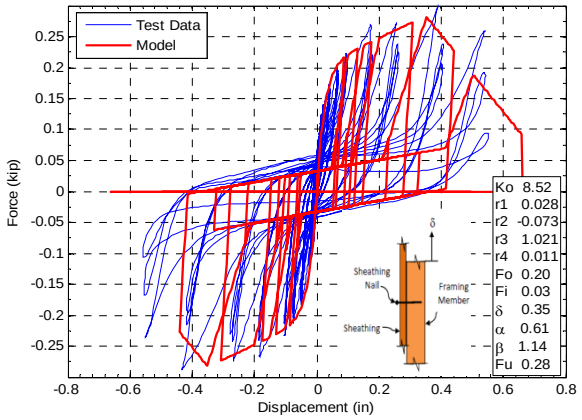

Figure 8. *Hysteretic model for sheathing nail.*

individual sheathing nails is usually negligible the rotational stiffness (k_r) of the sheathing nail was taken as zero.

3.5 Continuity Ties

Fig. 9 depicts the connection models for purlin-to-purlin and girder-to-girder with double-sided ties. The F2F element was used to model each continuity tie assembly. A continuity tie designed per the current code provisions within a collective chord model is expected to perform in the linear range [1]; therefore, a linear elastic spring oriented parallel to the tie's longitudinal direction was used to model the tie stiffness. The stiffness values of the linear elastic tie springs were obtained from the connection tests of three types of Simpson Strong-Tie continuity tie assemblies by Yarber [8]. The stiffness values along with the Simpson Strong-Tie product designations are given in Fig. 9. Note that the stiffness of the double-sided HD7B connection was found to be more than twice the stiffness of the single-sided HD7B connection. The stiffness of the single-sided HD7B connection was affected by bolt rotation. In this study, when modelling the double-sided connection, a pair of F2F elements was utilized and the stiffness of each of the F2F elements was taken as half of the value obtained from the double-sided test.

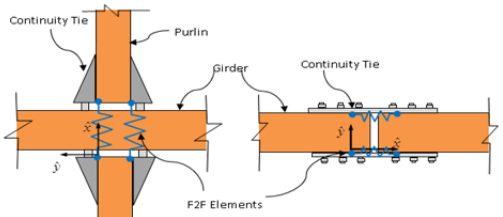

Connection Type	Stiffness (kip/in)
HDU-S2.5	67.57
HD7B (Single-sided)*	60.03
HD7B (Double-sided)*	229.06

* stiffness shown is for each single-sided HD7B or each double-sided HD7B.

Figure 9. *Continuity tie models for purlin-to-purlin and girder-to-girder connections.*

3.6 Subpurlin-to-purlin Connection Model

A pair of F2F elements was placed at each end of a subpurlin to model the connection between the subpurlin and purlin (i.e. the blocking to purlin connection). A bilinear elastic spring was used to model the relative displacement of the F2F connector in the local x-direction (Fig. 10). Compared to the stiffness of metal continuity ties at the purlin-to-girders, the withdrawal capacity of the subpurlin-to-purlin framing nail is very low and it has a negligible effect on the overall diaphragm behavior; hence, in the diaphragm models, when separation between the subpurlins and purlins occurred (i.e. for positive relative displacement), the stiffness of the x-spring was assumed to be zero. However, when contact occurred between the subpurlins and purlins, a high linear stiffness value (100 kip/in) was used to simulate the bearing contact effect. To allow for greater construction tolerances, gaps up to 1/8" are commonly provided between the subpurlin hangers and the purlins. In this study, the effect of gaps on the diaphragm behavior was not considered.

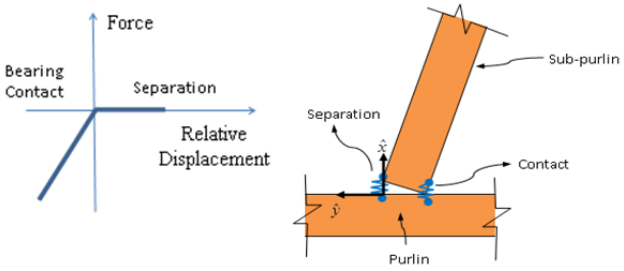

Figure 10. *Subpurlin-to-purlin contact model.*

4 CASE STUDY

A case study building with a panelized roof diaphragm system is provided herein to investigate the behavior of a panelized roof diaphragm and the assumptions used in the collective chord design method. The case study structure is a 96 ft x 192 ft (18,432 sf) single-story tilt-up concrete building (Fig. 11a) with open-space warehouse configuration and is assumed to be located in a seismically active zone along the west coast of the U.S. (Seismic Design Category D, Site Class D). The perimeter walls are 33 ft tall and 9 ¼" thick. The roof is a flat panelized all-wood roof system with OSB sheathing and located at 30 ft above the ground. The diaphragm is assumed to be constructed per the panelized construction method and each pre-framed panel unit is 24 ft x 8 ft (Fig. 9b). The girders are placed parallel to the longitudinal direction of the building and spaced at 24 ft on-center (o.c.). Purlins are spaced at 8 ft. o.c. supported by girders. Thus, each pre-framed panel is supported by purlins on two long sides and girders on the other two sides. The subpurlins (or stiffeners) are spaced at 2 ft o.c. The subpurlins and purlins are assumed to be constructed of visually graded Douglas Fir-Larch Select Structural sawn lumbers with a modulus of elasticity E =1900 ksi. Girders are assumed to be constructed of glulam (glued laminated timber) of stress class 24F-1.8E, with Douglas Fir laminates. The sheathing is made up of 4 ft x 8ft, 15/32" thick OSB with staggered layout (Fig. 11) and connected to the framing by 10d common nails. The dimensions of the purlins and girders were sized based on the gravity load design. The detailed calculations for seismic loads and gravity load design can be found in [9].

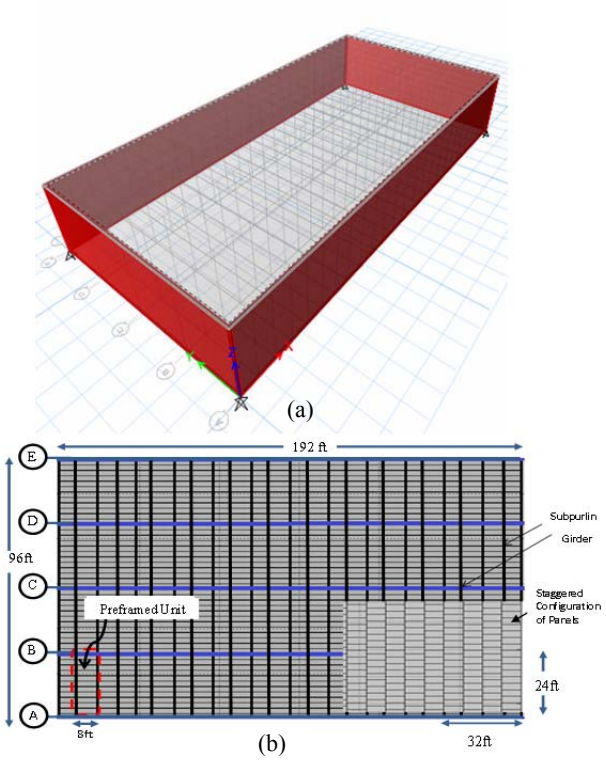

***Figure 11**. (a) A case study building model, and (b) panelized roof diaphragm model.*

***Table 1.** Study matrix for panelized roof diaphragm models.*

Model ID	Description	Connections											
		Panel-to-frame			Girder-to-Girder			Purlin-to-Girder			Subpurlin-to-Purlin		
		Nail Spacing	Model	Ko (k/in)	Type	Model	Ko (k/in)	Type	Model	Ko (k/in)	Type	Model	Ko (k/in)
BM	Benchmark model	Schedule I	MSTEW	8.52	HD7B Double	Bilinear Elastic	470	HD7B Double	Bilinear Elastic	470	Slip	Bi-Linear contact	0,100,100
MRPN	Model with rigid panel nails	Schedule I	Rigid	1.00E+05	HD7B Double	Bilinear Elastic	470	HD7B Double	Bilinear Elastic	470	Slip	Bi-Linear contact	0,100,100
A4:1	Model with aspect ratio 4:1	Schedule I	MSTEW	8.52	HD7B Double	Bilinear Elastic	470	HD7B Double	Bilinear Elastic	470	Slip	Bi-Linear contact	0,100,100
A1:2	Model with aspect ratio 1:2	Schedule I	MSTEW	8.52	HD7B Double	Bilinear Elastic	470	HD7B Double	Bilinear Elastic	470	Slip	Bi-Linear contact	0,100,100
MRFN	Model with rigid frame nails	Schedule I	MSTEW	8.52	HD7B Double	rigid	1.00E+05	HD7B Double	rigid	1.00E+05	Slip	Bi-Linear contact	0,100,100
L2	Model with load pattern 2	Schedule I	MSTEW	8.52	HD7B Double	Bilinear Elastic	470	HD7B Double	Bilinear Elastic	470	Slip	Bi-Linear contact	0,100,100
L3	Model with load pattern 3	Schedule I	MSTEW	8.52	HD7B Double	Bilinear Elastic	470	HD7B Double	Bilinear Elastic	470	Slip	Bi-Linear contact	0,100,100
M2.5/2.5	Uniform panel nail spacing of 2.5"o.c	Schedule III	MSTEW	8.52	HD7B Double	Bilinear Elastic	1.00E+05	HD7B Double	Bilinear Elastic	1.00E+05	Slip	Bi-Linear contact	0,100,100
M4/4	Uniform panel nail spacing of 4" o.c.	Schedule II	MSTEW	8.52	HD7B Double	Bilinear Elastic	1.00E+05	HD7B Double	Bilinear Elastic	1.00E+05	Slip	Bi-Linear contact	0,100,100
M2.5/4	Nail spacing 2.5"/4"	Schedule IV	MSTEW	8.52	HD7B Double	Bilinear Elastic	1.00E+05	HD7B Double	Bilinear Elastic	1.00E+05	Slip	Bi-Linear contact	0,100,100
M4/6	Nail spacing 4"/6"	Schedule V	MSTEW	8.52	HD7B Double	Bilinear Elastic	1.00E+05	HD7B Double	Bilinear Elastic	1.00E+05	Slip	Bi-Linear contact	0,100,100
Mmult	Multiple nail zones	Multiple Nail Zones	MSTEW	8.52	HD7B Double	Bilinear Elastic	1.00E+05	HD7B Double	Bilinear Elastic	1.00E+05	Slip	Bi-Linear contact	0,100,100

•BM-L3: 10d common nails at a spacing of 6"o.c. throughout the panel edges, 12"o.c for intermediate field nailing
•M2.5/2.5-Mmult: 10d common nails at a spacing of 12"o.c for intermediate field nailing
•Nail Schedule I: 6"o.c. boundaries & continuous edges, 6"o.c. other edges, 12"o.c. intermediate field area
•Nail Schedule II: 4"o.c. boundaries & continuous edges, 6"o.c. other edges, 12"o.c. intermediate field area
•Nail Schedule III: 2.5"o.c. boundaries & continuous edges, 4"o.c. other edges, 12"o.c. intermediate field area
•Nail Schedule IV: 2.5"o.c. boundary and continuous edges, 4"o.c. other edges
•Nail Schedule V: 4"o.c. boundary and continuous edges, 6"o.c. other edges

5 Select Modeling Results

Twelve models were created using the M-CASHEW program to analyze the behavior of the case study roof diaphragm discussed in the previous section. Table 1 shows the parameters for each model. As stated previously, the overall diaphragm behavior is mainly governed by the connections. Hence, in this study, the dimensions and properties of the sheathing and framing members were kept constant. The model designated as BM is the benchmark model, which has modeling parameters that most closely represent the actual behavior of the case study diaphragm. The sheathing nails were modeled using the nonlinear MSTEW hysteretic model (see Fig. 8). The axial stiffness of the continuity ties (girder-to-girder and purlin-to-purlin) were based on the stiffness values obtained from continuity tie tests by Yarber [8] (see Fig. 9).

Sensitivity studies were performed by modifying the benchmark model (*BM*) and changing the modeling parameters one at a time to investigate the influence of different modeling parameters on the overall behavior of panelized roof diaphragms. Three different load patterns were considered to represent the effect of wind and earthquake loadings. Load Pattern I was a uniform in-plane load, which was used to represent the lateral inertia load induced by an example earthquake. Load Pattern II had one line of uniform load applied along one edge of the diaphragm (windward force), and Load Pattern III had two line loads applied to two opposite edges in the same direction (windward and leeward wind forces).

It should be noted that the benchmark model *BM* had a uniform nailing schedule. Multiple nail zones are common in large diaphragm construction. The effect of the sheathing nailing schedule on the diaphragm behavior was also analyzed. Models *BM*, *M2.5/2.5* and *M4/4* had uniform edge nail spacing throughout the diaphragm, whereas Models *M2.5/4* and *M4/6* had different edge nail spacings for the boundary and continuous edges. Model *Mmult* had multiple nail zones. While twelve models were analyzed only selected results are presented in this paper. The complete results may be found in [9].

5.1 Chord Force Distribution

The pushover curve for the benchmark model BM is shown in Fig 12. The displacement shown is measured at the mid-span of the diaphragm and the force is the sum of the reaction forces at the supports. As expected, the pushover curve is nonlinear. This is mainly attributed to the nonlinear shear slip behavior of the sheathing nails.

The axial force distributions in the chord members at mid-span when the displacement is 1 in. (linear segment of pushover curve) and 6.8 in. (end of pushover curve, nonlinear stage) are shown in Fig. 12b and 12c, respectively. The results show that the axial forces are mainly carried by the exterior chords. The values next to the horizontal bars show the axial force magnitudes as a fraction of the maximum axial force carried by the exterior chord in tension. According to the modeling results, the initial tension force in the girder line at one quarter of the diaphragm width, measured from the tension side of the diaphragm, is approximately 10% of that carried by the end chord (Fig. 12b). At the diaphragm's nonlinear stage, the tension force in this girder line reduces to approximately 4% of the extreme tension chord (Fig. 12c).

Note that the magnitudes of tension and compression forces in the two exterior chords are not identical. Fig. 12b and Fig. 12c show that the maximum compression forces at linear and nonlinear stages are 91% and 92% of that in the extreme tension chord. From the distribution of the axial forces across the depth of the diaphragm, one can see that the neutral axis is located slightly below the mid-depth of the diaphragm and is closer to the exterior chord in compression than in tension. This is because the subpurlins on the compression side of the neutral axis are in bearing

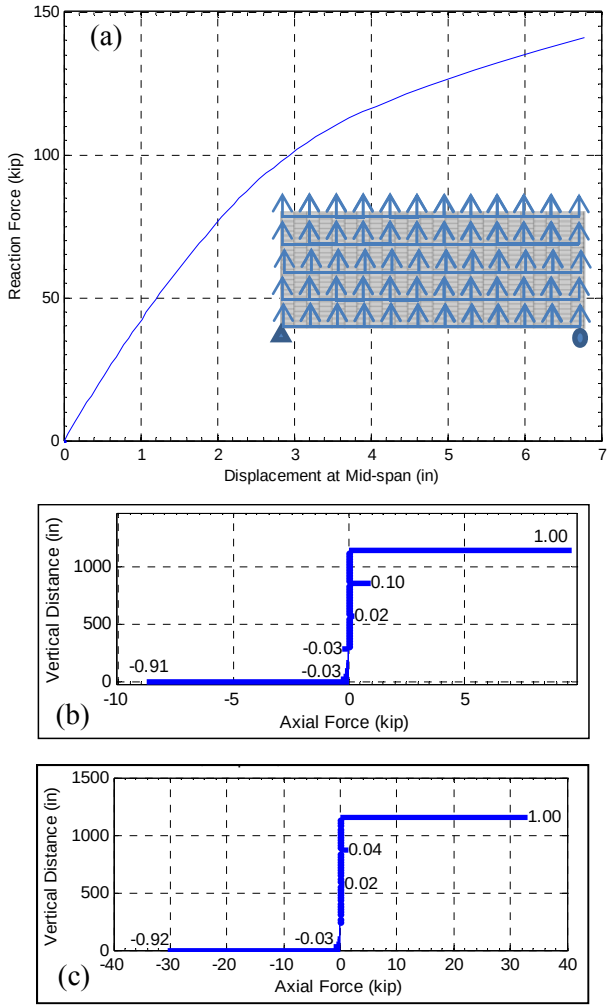

Figure 12. *(a) Lateral pushover curve of benchmark diaphragm model (BM); chord force distributions at mid-span when the pushover displacement is (b) 1 in. and (c) 6.8 in.*

contact with the purlins and are carrying some axial forces. On the other hand, separations between the subpurlins and purlins occur for those subpurlins on the tension side of the neutral axis. Since the subpurlins do not have continuity ties, no tension forces are carried by these subpurlin lines. While no tension forces are transferred by the subpurlins, the sheathing nails above the subpurlins can carry both tension and compression forces in the sheathing.

5.2 Diaphragm Aspect Ratio

The axial force distributions for three diaphragms with different aspect ratios (length-to-width ratios of 0.5, 2 and 4) are compared in Fig. 13. Since the length of these three diaphragms are not identical, in order to compare their results, the chord forces and chord locations are normalized. The chord forces are normalized by dividing the axial force in each chord of a diaphragm by the maximum chord force for the given diaphragm. The locations of chords are normalized by dividing it by the distance between the extreme chords (i.e. the width of the diaphragm). As can be seen from Fig. 13, as the aspect ratio of the diaphragm increases, the participation of interior chords in carrying axial load also increases. It can also be observed in Fig. 13 that the interior chords towards the exterior sides carry more load than those chords towards the middle. However, as discussed previously, the forces carried by the interior chords are still not comparable to the forces predicted by the collective chord method (solid blue line). In fact, for the range of diaphragm aspect ratios considered, the collective chord method overestimates the forces carried by the interior chords. This indicates that, in order to use the collective chord method, a modification factor applied to the distribution of the interior chord forces is needed. Alternatively, the traditional diaphragm design method can be conservatively used to determine the exterior chord forces.

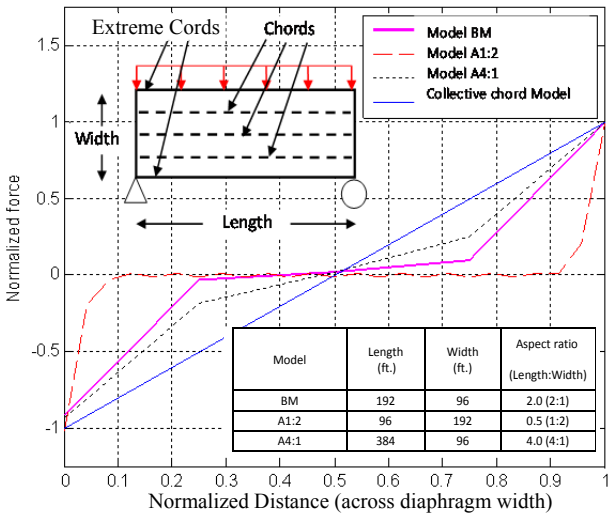

Figure 13. *Distribution of chord forces for diaphragms of different aspect ratios.*

6 SUMMARY AND CONCLUSION

Based on the modeling results, it was observed that the distribution of chord forces is a function of the diaphragm aspect ratio. As the diaphragm aspect ratio (length-to-width) reduces, the chord force distribution approaches the assumption speculated in the traditional diaphragm design method. For high aspect ratio diaphragms, the chord force distribution approaches the collective chord model predictions. However, in the range of aspect ratios typical to large panelized roof diaphragms, it was observed that the collective chord method over-predicted the chord forces carried by the intermediate chords and under-predicted the chord forces carried by the two exterior chords. Since the accuracy of the collective chord method is dependent upon the diaphragm's aspect ratio, an aspect ratio dependent modification factor applied to the distribution of the chord forces may be needed.

ACKNOWLEDGEMENTS

This material is based upon work partially supported by FPInnovations. Any opinions, findings, and conclusions or recommendations expressed in this material are those of the investigators and do not necessarily reflect the views of FPInnovations. A sincere thank you to Ciprian Pirvu for providing diaphragm test data [10] used in this study for verifying the numerical models.

REFERENCES

[1] Lawson JW, Yarber CN. Collective chord behavior in large flexible diaphragms. *Proceeding of 2013 Structures Congress*, Pittsburg, PA, 2013.

[2] Bender AD, Gebremdehin KG, Pollock DG. Designing for chord in post frame roof diaphragms. *Frame Building News*, 40-44, 1996.

[3] Lawson JW. Thinking outside the box: new approaches to very large flexible diaphragms, *Proceeding of SEAOC 2007 Convention*, 2007.

[4] Pang W., Shirazi SMH. Corotational model for cyclic analysis of light-frame wood shear walls and diaphragms. *ASCE Journal of Structural Engineering* 2013; **139** (8): 1303-1317.

[5] Judd JP. *Analytical modeling of wood frame shear walls and diaphragms*. Master's Thesis, Brigham Young University, Provo, UT, 2005.

[6] Folz B, Filiatrault A. Cyclic analysis of wood shear walls, *ASCE Journal of Structural Engineering*; 2001; **27**(4): 434-441.

[7] Ekiert C, Hong J. *Framing-to-sheathing connection tests in support of NEESWood Project*. Network of Earthquake Engineering Simulation. State University of New York at Buffalo, Buffalo, NY, 2006.

[8] Yarber CN. *Experimental determination of the stiffness and strength of continuity tie connections in large wood roof diaphragms and impact on the collective chord model*, Master's Thesis, California Polytechnic State University, San Luis Obispo, CA, 2012.

[9] Pant S. *Numerical study of the structural performance of large panelized all-wood roof diaphragms*, Master's Thesis, Clemson University, Clemson, SC, 2013.

[10] Pirvu, C. (2008). *Structural Performance Of Wood Diaphragms With Thick Panels*, FPInnovations FORINTEK, Project No. 4636.